# Resource Allocation for Multicarrier D2D Video Transmission Based on Exact Symbol Error Rate

Peizhi Wu, Pamela C. Cosman, and Laurence B. Milstein
Department of Electrical and Computer Engineering,
University of California, San Diego, USA
Email: peizhiwu@ucsd.edu, pcosman@eng.ucsd.edu, milstein@ece.ucsd.edu

*Abstract*—We consider centralized cross-layer resource allocation for a device-to-device (D2D) video transmission system, given knowledge of the channel state information and the rate distortion information of the video streams, and propose an iterative algorithm for subcarrier assignment and power allocation. In the resource allocation, the performance improvement by applying the exact symbol error rate (SER) is compared with the conventional signal-to-interference-plus-noise-ratio (SINR) based SER evaluation method that uses a Gaussian approximation (GA) for the aggregated interference. An exact SER expression for a D2D system using multicarrier bandlimited QAM is derived and then used in the resource allocation algorithm. Bit-level simulations for different numbers of D2D pairs demonstrate a considerable improvement on user capacity and video peak signal-to-noise ratio by incorporating the proposed SER expression compared to the GA.

*Index Terms*—Device-to-device communication, multimedia communication, radio spectrum management, cochannel interference.

## I. INTRODUCTION

Device-to-device (D2D) communication [1] is a communications paradigm that allows multiple transmitter-receiver pairs to share the same spectrum, thereby improving the spectral efficiency and offloading traffic from the base station. Since a D2D user operating on shared spectrum receives not only the desired signal but also signals from other users, cochannel interference (CCI) is produced and is a key consideration in the design of a D2D communication system. The interference signals may not be synchronized at every D2D receiver [2] due to the propagation delay between multiple D2D pairs, so the inter-carrier interference (ICI) caused by the high out-of-band (OOB) emission of orthogonal frequency division multiplexing (OFDM) [3] poses a challenge. In this context, Filter Bank Multicarrier (FBMC) based waveforms that use bandlimited pulse shapes, such as Filtered Multi-tone (FMT) [4], have been evaluated as candidates for the waveforms of D2D communications.

A well-known approach to treating the interference is the Gaussian approximation (GA), which treats the aggregated CCI as a Gaussian random variable. For example, a few literature on the resource allocation for D2D systems [5]–[8] considered the optimization for the weighted sum rate of D2D pairs using the capacity of Gaussian channels, which was

based on treating the interference by the GA. However, the GA heavily relies on the conditions that validate the central limit theorem, which may not be suitable for D2D systems. First, the spectrum of D2D systems is shared by users without the use of spread spectrum, so the number of interfering users can be small [9]. Also, one or a few of the interferers may have significantly larger power than others at a D2D receiver.

Current multimedia applications often use quadrature amplitude modulation (QAM) for rate-adaptive transmission [10], due to its practicality and bandwidth efficiency. To circumvent the GA, an analytical expression of the exact symbol error rate (SER) of bandlimited QAM under CCI that applies to the D2D systems is of great interest. Early endeavors to calculate the error rate in a bandlimited system with interference were devoted to phase-shift keying (PSK) [11]–[14]. Nevertheless, unlike PSK, the symbols of high-order QAM, such as 16-QAM or 64-QAM, have multiple power levels, and the treatments for PSK modulated CCI in [11]–[14] are not applicable to QAM modulated CCI. Few papers were related to the error rate of bandlimited QAM corrupted by CCI, including saddlepoint integration [15] and numerical integration [16]. Neither of [15], [16] provided an analytical expression for the error rate, thereby were unsuitable for use in resource allocation.

Previous centralized resource allocation for D2D systems, such as [5]–[8], divided the spectrum into frequency-flat subcarriers and restricted every D2D user's access to the spectrum of a single subcarrier. Nevertheless, to fully exploit frequency diversity, D2D users can be assigned to multiple subcarriers, and the resultant optimization problem with a total power constraint resembles the discrete dynamic spectrum management (DSM) problem [17], [18]. For the multicarrier and multiuser setting, the discrete DSM problem was shown to be generally non-convex and thereby to be NP-hard [18].

For video delivery with delay constraints, forward error correction (FEC)-based transmission with no retransmission is usually used [19], which demands a low packet loss rate [20] or a low SER [21]. In [21], a cross-layer resource allocation algorithm for video transmission on cellular uplinks was proposed, in which every subcarrier was assigned to a single user. However, for D2D systems, a subcarrier can be assigned to multiple users to improve spectral efficiency. Literature on resource allocation for D2D video delivery included optimization for energy efficiency subject to a QoS constraint [22], and for a utility function that was jointly determined by
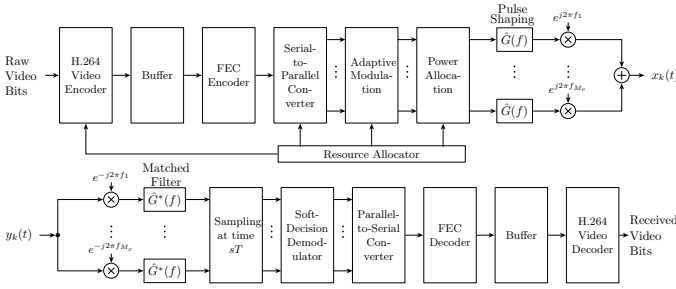
Fig. 1: Block diagram of the transceiver.

the throughput and transmission power [23]. Optimization for overall video quality of D2D transmission does not appear to have been addressed.

This paper is organized as follows. Section II describes the system model. Section III derives an analytical expression for the SER of bandlimited QAM under CCI. In Section IV, the optimization problem for resource allocation in multicarrier D2D video transmission systems is formulated, and an iterative subcarrier and power allocation algorithm is proposed. Section V presents simulation results, and compares the performance of the proposed algorithm with the performance of the same algorithm using the SER obtained by the GA. Section VI contains the conclusion remarks.

## II. SYSTEM MODEL

Consider a single cell D2D video transmission system served by a base station (BS). There are $K$ pairs of D2D users in the cell. Each D2D pair consists of a transmitter and a receiver, with a D2D link from the transmitter to the receiver. The system allocates a total frequency band of $W$ (Hz), which is equally divided into $M_c$ orthogonal subcarriers, exclusively to these D2D pairs [24]. Each D2D pair has access to any of these subcarriers subject to the subcarrier and power allocation by the BS. The system operates in a time-slot manner. We consider video delivery with a delay constraint, for which one group of pictures (GOP) is transmitted in a time slot. The duration of a GOP, denoted by $T_{\text{GOP}}$, is a constant. The subcarrier assignment and power allocation decision is made by the BS at the beginning of each GOP. We assume perfect channel estimation for the desired and interfering signals at receivers, and the BS is able to collect the channel state information (CSI) and video rate-distortion (RD) information via the control channels without error.

### A. Transceiver Architecture

The transceiver adopts a multicarrier architecture, whose block diagrams are given in Fig. 1. The FEC protected video sequences are mapped to the subcarriers as complex-valued modulated symbol sequences at a symbol rate of $1/T$. The signal on the $m$-th subcarrier of the $k$-th transmitter is modulated by $M_{k,m}$-ary QAM, where the $\{\sqrt{M_{k,m}}\}$ are positive even integers. The $s$-th complex modulated symbol on the $m$-th subcarrier of the $k$-th transmitter is denoted by $X_k^{(m)}[s]$, whose variance is normalized to unity. The impulse response

of the pulse shaping filter is denoted by $\hat{g}(t)$, whose energy is normalized to unity, i.e. $\int_{-\infty}^{\infty} [\hat{g}(t)]^2 = 1$. The lowpass equivalent signal for the $k$-th transmitter is given by

$$x_k(t) = \sum_{m=1}^{M_c} \sqrt{p_{k,m}T} \sum_s X_k^{(m)}[s]\, \hat{g}(t-sT)\, e^{j2\pi f_m t}, \quad (1)$$

where $p_{k,m}$ is the transmission power on the $m$-th subcarrier of the $k$-th D2D transmitter, and the central frequency of the $m$-th subcarrier is denoted by $f_m = W(m-1/2)/M_c$. A root-raised-cosine filter $\hat{g}(t)$ with roll-off factor $0 < \beta \le 1$ is used for pulse shaping, whose frequency response $\hat{G}(f)$ is [25]:

$$\hat{G}(f) = \sqrt{\frac{T}{2}\left\{1 - \cos\left[\pi \lin_\beta\left(Tf\right)\right]\right\}}, \quad (2)$$

where $\lin_\beta(x) = \min(1, \max(0, ((1+\beta)/(2\beta)) - (|x|/\beta)))$ is used to systematically describe the roll-off area defined by $\beta$ in the frequency domain [25]. The pulse shaping filter $\hat{G}(f)$ has a bandwidth of $(1+\beta)/(2T)$. The system adopts an FMT waveform [4], in which the spectra of adjacent subcarriers do not overlap, namely $(1 + \beta)/T \le W/M_c$, so ICI does not exist. The cascade of the pulse shaping and matched filter $G(f) = |\hat{G}(f)|^2$ manifests to a raised-cosine (RC) pulse [26], therefore, ISI does not exist if there is perfect bit synchronization. The inverse Fourier transform of $G(f)$ is $g(t) = \text{sinc}\,(\pi t/T) \cdot \cos\,(\pi \beta t/T)/(1 - 4\beta^2 t^2/T^2)$ [26].

The interference from the $i$-th transmitter arrives at the $k$-th receiver with a channel gain $|h_m^{i,k}|$, a time delay $\tau_i^{(k)}$ and a phase delay $\phi_i^{(k)}$ compared to the desired signal from the $k$-th transmitter ($i, k \in \{1, 2, \cdots, K\}$), where $\phi_i^{(k)}$ is uniformly distributed in $[0, 2\pi)$ and $\tau_i^{(k)}$ modulo $T$ is uniformly distributed in $[0, T)$, if $i \ne k$. Also, $|\tau_i^{(k)}| \ll T_{\text{GOP}}$. We assume that a coherent receiver is implemented, which maintains perfect bit synchronization and phase recovery for the desired signal, so we set $\tau_k^{(k)} = 0$ and $\phi_k^{(k)} = 0$. We further assume that the channel gain $|h_m^{i,k}|$ is unchanged for the duration of a time slot. Therefore, the lowpass equivalent signal at the $k$-th receiver is given by

$$y_k(t) = \sum_{m=1}^{M_c} \sum_{i=1}^{K} \sqrt{P_i^{(k,m)}T} \sum_s X_k^{(m)}[s]\, \hat{g}(t - \tau_i^{(k)} - sT)$$
$$\cdot e^{j(2\pi f_m t + \phi_i^{(k)})} + n_k(t), \quad (3)$$

where $P_i^{(k,m)} = p_{i,m}|h_m^{i,k}|^2$ is the power of the $i$-th signal received on the $m$-th subcarrier of the $k$-th D2D receiver prior to demodulation, and $n_k(t)$ is complex Additive White Gaussian Noise (AWGN) at the $k$-th receiver with two-sided power spectral density $N_0$. As shown in Fig. 1, a matched filter is implemented at each subcarrier of the receiver, so the output for the $s$-th symbol is given by $Y_k^{(m)}[s] = \int_{-\infty}^{\infty} y_k(t)\hat{g}(t - sT)\exp(-j2\pi f_m t)dt$. Without loss of generality, we consider the reception of the 0-th symbol. The decision statistic at the output of the matched filter of the receiver for the 0-th symbol

can be written as

$$Y_k^{(m)}[0] = \sqrt{P_k^{(k,m)}T}\, X_k^{(m)}[0] + \sum_{i=1,i\neq k}^{K} \sqrt{P_i^{(k,m)}T}\, e^{j\phi_i^{(k)}}$$

$$\cdot \sum_s X_i^{(m)}[s]\, g(-\tau_i^{(k)} - sT) + N_k^{(m)}[0], \qquad (4)$$

where the first term is the desired signal component, and the second term represents the CCI components. The noise term is given by $N_k^{(m)}[s] = \int_{-\infty}^{\infty} n_w(t)\hat{g}(t-sT)dt$, which is a zero-mean complex circularly symmetric Gaussian random variable (RV) with power $P_N = N_0 \int_{-\infty}^{\infty} [\hat{g}(t)]^2 dt = N_0$. The signal-to-noise ratio (SNR) and the signal-to-interference ratio (SIR) on the $m$-th subcarrier of the $k$-th receiver can be expressed as $\mathrm{SNR}_{k,m} = 10\log_{10}\left[p_{k,m}|h_m^{k,k}|^2/(N_0/T)\right]$ and $\mathrm{SIR}_{k,m} = 10\log_{10}[p_{k,m}|h_m^{k,k}|^2/(\sum_{i=1,i\neq k}^{K} p_{i,m}|h_m^{i,k}|^2)]$, respectively.

### B. Scalable Video Codec

The D2D videos are encoded with the scalable video coding (SVC) extension of H.264/AVC with medium granular scalability (MGS) [27]. The mean square error (MSE) of the video diminishes as more video bits are successfully delivered. The video packets are transmitted in the order of descending priority. If an error occurs during transmission, that packet and all successive packets in the GOP will be dropped, but previous packets will be used for decoding the GOP. The RD curve of the video characterizes the tradeoff between the video distortion and the number of bits used to compress the raw video data. Since the video is compressed on a GOP-by-GOP basis, this RD function is also measured for each GOP. The MSE distortion $D_k$ can be approximated as a function of the number of correctly received video bits $B_k$ in a GOP, written as $D_k = v_k + u_k'/(B_k + w_k')$ [28], where $v_k$, $u_k'$, and $w_k'$ depend on video content and are positive constants determined by curve fitting. The video bits are protected by an FEC code with fixed rate $r$. The number of video bits transmitted in a GOP on link $k$ is given by $B_k = (rT_{\mathrm{GOP}}/T)\sum_{m=1}^{M_c}\log_2(M_{k,m})$. For simplicity, define $u_k = u_k'T/(rT_{\mathrm{GOP}})$, $w_k = w_k'T/(rT_{\mathrm{GOP}})$, then the total MSE of the GOPs at the video decoders for all D2D pairs can be further written as

$$D_{\mathrm{total}} = \sum_{k=1}^{K}\left(v_k + \frac{u_k}{\sum_{m=1}^{M_c}\log_2(M_{k,m}) + w_k}\right). \qquad (5)$$

When the same number of additional video bits are received, a GOP with a steeper slope on the RD curve generates a larger decrease in video MSE. The slope of the RD curve evaluated at the assigned alphabet sizes is given by [21]

$$S_k = -\frac{u_k}{(\sum_{m=1}^{M_c}\log_2(M_{k,m}) + w_k)^2}. \qquad (6)$$

### III. SYMBOL ERROR RATE FOR D2D RECEIVERS

In this section, we consider the SER for the $m$-th subcarrier of the $k$-th D2D receiver. From (4), the aggregated CCI in the

decision statistic is given by

$$I_{k,m} = \sum_{i=1,i\neq k}^{K}\sqrt{P_i^{(k,m)}T}\, e^{j\phi_i^{(k)}}\sum_{s=-\infty}^{\infty} X_i^{(m)}[s]\, g(-\tau_i^{(k)} - sT). \qquad (7)$$

### A. SER Evaluation by the GA

The GA treats the aggregated CCI as a zero-mean complex circularly symmetric Gaussian RV with the same variance. The variance of the aggregated CCI is given by

$$\mathrm{Var}(I_{k,m}) = \sum_{i=1,i\neq k}^{K} P_i^{(k,m)}T \cdot E\left[\sum_{s=-\infty}^{\infty} g^2(-\tau_i^{(k)} - sT)\right] \qquad (8)$$

where the $E[\sum_{s=-\infty}^{\infty} g^2(-\tau_i^{(k)} - sT)] = 1 - \beta/4$ for a RC pulse with roll-off factor $\beta$ [12, (55)]. With the GA, the SER evaluation resembles the well-known SER expression for QAM in AWGN, which depends on the signal-to-interference-plus-noise ratio (SINR). The SER of $M_{k,m}$-ary QAM with CCI using the GA is thus given by [29]

$$\mathrm{SER}_{k,m}^{\mathrm{GA}} = 4\mu_{k,m}Q\left(\sqrt{\frac{3\,\gamma_{k,m}}{M_{k,m}-1}}\right) - 4\mu_{k,m}^2 Q^2\left(\sqrt{\frac{3\,\gamma_{k,m}}{M_{k,m}-1}}\right), \qquad (9)$$

where $\mu_{k,m} \triangleq 1 - 1/\sqrt{M_{k,m}}$ and the SINR is given by

$$\gamma_{k,m} = \frac{p_{k,m}|h_m^{k,k}|^2}{(1-\frac{\beta}{4})\sum_{i=1,i\neq k}^{K} p_{i,m}|h_m^{i,k}|^2 + \frac{N_0}{T}}. \qquad (10)$$

### B. Exact SER in the Form of a Power Series

To assess the accuracy of the GA in the SER evaluation for D2D systems, we derive the exact expression for the SER of the bandlimited QAM under CCI and only list the results here. The derivation for the SER expression and the truncation error is omitted due to limited space and can be found in [30].

We first present in Proposition 1 a power series expansion for the joint CF of $I_{k,m}^I$ and $I_{k,m}^Q$, where $I_{k,m}^I \triangleq \mathrm{Re}[I_{k,m}]$ and $I_{k,m}^Q \triangleq \mathrm{Im}[I_{k,m}]$ are the in-phase and quadrature components of the aggregated CCI, respectively.

*Proposition 1:* The power series expansion of the joint CF of $I_{k,m}^I$ and $I_{k,m}^Q$ is given by

$$\varphi_{I_{k,m}^I,I_{k,m}^Q}(u,v) = \sum_{n=0}^{\infty} b_n^{(k,m)}(-N_0)^n(u^2+v^2)^n, \qquad (11)$$

where $b_0^{(k,m)} = 1$ and the recursive relation of $\{b_n^{(k,m)}\}$ for $n = 1, 2, \cdots$ is given by

$$b_n^{(k,m)} = \sum_{p=1}^{n} \frac{p}{n} b_{n-p}^{(k,m)} \sum_{i=1,i\neq k}^{K} \left(\frac{P_i^{(k,m)}T}{N_0}\right)^p d_p^{(M_{i,m})}. \qquad (12)$$

In (12), $d_0^{(M_{i,m})} = 0$ and the following recursive relationship holds for positive integer $n$:

$$d_n^{(M_{i,m})} = \alpha_n^{(M_{i,m})} - \sum_{p=1}^{n-1} \frac{p}{n} d_p^{(M_{i,m})}\alpha_{n-p}^{(M_{i,m})}. \qquad (13)$$

$$\text{SER}_{k,m}^{(2L)} = 4\mu_{k,m}Q(\sqrt{2}\nu_{k,m}) - 4\mu_{k,m}^2\left[Q(\sqrt{2}\nu_{k,m})\right]^2 + \frac{4\mu_{k,m}}{\sqrt{\pi}}e^{-\nu_{k,m}^2}\left[1 - 2\mu_{k,m}Q(\sqrt{2}\nu_{k,m})\right]\sum_{l=1}^{L-1}b_l^{(k,m)}H_{2l-1}(\nu_{k,m})$$

$$- \frac{4\mu_{k,m}^2}{\pi}e^{-2\nu_{k,m}^2}\sum_{n=1}^{L-1}\sum_{p=1}^{n-1}b_n^{(k,m)}\binom{n}{p}H_{2p-1}(\nu_{k,m})H_{2(n-p)-1}(\nu_{k,m}), \tag{18}$$

---

In (13), $\{\alpha_n^{(M)}\}$ are a set of coefficients given by

$$\alpha_n^{(M)} = \left(\frac{3}{M-1}\right)^n\sum_{p=0}^{n}B_{2p,2(n-p)}\sum_{q=0}^{2n}\sum_{q_1=0}^{q}B_{q_1,q-q_1}\sum_{q_2=\max(0,q+2p-2n)}^{\min(q,2p)}$$

$$\cdot\sum_{q_3=\max(0,q_1+q_2-q)}^{\min(q_1,q_2)}z_p^{(M)}(q_2,q_3)z_{n-p}^{(M)}(q-q_2,q_1-q_3), \tag{14}$$

where $B_{m,n} = (m-1)!!(n-1)!!/[(m+n)!!]$ if $m \geq 0$, $n \geq 0$, $m,n$ both even, and $B_{m,n} = 0$ otherwise. Note that $(2n-1)!! = 1\cdot3\cdots(2n-1)$, $(2n)!! = 2\cdot4\cdots2n$ for any positive integer $n$, and $0!! = (-1)!! = 1$.

The recursive relations for $\{z_n^{(M)}(q,q_1)\}$ in (14) are given by

$$z_n^{(M)}(q,q_1) = \sum_{p=1}^{n}\frac{p}{n}c_p^{(M)}\sum_{q_2=\max(0,q+2p-2n)}^{\min(q,2p)}\sum_{q_3=\max(0,q_1+q_2-q)}^{\min(q_1,q_2)}R_p(q_2,q_3)$$

$$\cdot z_{n-p}^{(M)}(q-q_2,q_1-q_3), \tag{15}$$

for $n \geq 1$, $0 \leq q_1 \leq q \leq 2n$ and $z_0^{(M)}(0,0) = 1$.

Let $G_{2n}(f)$ be the Fourier transform of $[g(t)]^{2n}$, given by $G_{2n}(f) \triangleq \int_{-\infty}^{\infty}[g(t)]^{2n}\cos(2\pi ft)\,dt$. Also, let $\epsilon_q = 1$ for $q = 0$ and $\epsilon_q = 2$ otherwise. The expression for coefficients $\{R_n(q,q_1)\}$ in (15) is given by

$$R_n(q,q_1) = \frac{\epsilon_q}{T}\binom{q}{q_1}(-1)^{\frac{q_1}{2}}G_{2n}\left(\frac{q}{T}\right), \tag{16}$$

for $q_1$ even, $0 \leq q_1 \leq q \leq 2n$, and $R_n(q,q_1) = 0$ otherwise.

Also, the recursive relations for coefficients $\{c_n^{(M)}\}$ in (15) are given by $c_0^{(M)} = 0$ and for $n = 1, 2, \cdots$

$$c_n^{(M)} = a_n^{(M)} - \sum_{p=1}^{n-1}\frac{p}{n}c_p^{(M)}a_{n-p}^{(M)}, \tag{17}$$

where $a_n^{(M)} = 2/[(2n)!\sqrt{M}]\sum_{l=1}^{\sqrt{M}/2}(2l-1)^{2n}$ for $n = 0, 1, \cdots$.

*Proof:* The proof is by averaging over $\tau_i^{(k)}$ and $\phi_i^{(k)}$ and is omitted here due to limited space. ∎

As a remark, $\{d_n^{(M_{i,m})}\}$ is a set of coefficients that are determined only by the alphabet size and the pulse shape, then do not depend on the signal power, and thereby can be calculated offline.

We only use a finite number of terms from the power series in (11) to calculate the SER. After some manipulations using Proposition 1, retaining the terms with order less than $2L$ from $\varphi_{I_{k,m}^I,I_{k,m}^Q}(u,v)$ in the SER evaluation, where $L$ is a positive integer, the truncated evaluation for the SER is given

by (18), where $\nu_{k,m} \triangleq \sqrt{3p_{k,m}|h_m^{k,k}|^2T/[2N_0(M_{k,m}-1)]}$, $\mu_{k,m} \triangleq 1 - 1/\sqrt{M_{k,m}}$, and $H_n(x)$ is the $n$-th Hermite Polynomial with the following recursive relation [31, 8.95]: $H_0(x) = 1$, $H_1(x) = 2x$ and $H_{n+1}(x) = 2xH_n(x) - 2nH_{n-1}(x)$ for $n = 2, 3, \cdots$.

By comparing $\text{SER}_{k,m}^{(2L)}$ in (18) and the exact SER ($\text{SER}_{k,m}^{\text{exact}} = \lim_{L\to\infty}\text{SER}_{k,m}^{(2L)}$), a truncation error is introduced. An upper bound for the truncation error is given by

$$|\text{SER}_{k,m}^{(2L)} - \text{SER}_{k,m}^{\text{exact}}|$$

$$< \frac{1}{M_{k,m}}\sqrt{\frac{6p_{k,m}|h_m^{k,k}|^2}{\pi N_0/T}}\left(C\sum_{i=1,i\neq k}^{K}\sqrt{\frac{6p_{i,m}|h_m^{i,k}|^2}{N_0/T}}\right)^{2L}$$

$$\cdot\left(\sqrt{\frac{6p_{k,m}|h_m^{k,k}|^2}{\pi N_0/T}}\frac{1}{(2L-1)!!} + \frac{2}{(2L)!!}\right) \tag{19}$$

where $L$ is a positive integer, and $C = \max_{0<\tau<T}\sum_{s=-\infty}^{\infty}|g(\tau - sT)|$ is a positive, finite constant dependent on the pulse shape. For example, $C = 10\sqrt{2}/(3\pi)$ for a RC pulse with roll-off factor $0.5$. Notice that $|\text{SER}_{k,m}^{(2L)} - \text{SER}_{k,m}^{\text{exact}}| \to 0$ as $L \to \infty$. Therefore, the truncated series in (18) converges to the exact SER as more terms are used in the calculation.

## IV. ITERATIVE RESOURCE ALLOCATION ALGORITHM

### A. Problem Formulation

The objective of resource allocation is to minimize the total video MSE of all D2D pairs. The BS collects the video RD information and the CSI of all D2D pairs, and allocates subcarriers and transmission power to D2D pairs based on both the RD functions and the CSI.

Recall that the transmission power and the alphabet size of the $k$-th D2D pair on subcarrier $m$ are denoted by $p_{k,m}$ and $M_{k,m}$, respectively. We denote the set of supported alphabet sizes by $\mathcal{M}_{\mathcal{A}} = \{\mathcal{M}_1, \cdots, \mathcal{M}_{N_A}\}$. Each D2D transmitter is subject to a total power constraint $P$. In the power allocation procedure, the BS sets a fixed target for the SER on every D2D link and assumes error-free transmission in the resource allocation algorithm if the SER target is satisfied[1]. The video

---

[1]This error-free assumption is only used in determining the subcarrier assignment and power allocation. In the simulation, an error may still occur even if the SER target is satisfied.

MSE minimization problem is formally written as

$$\text{minimize} \sum_{k=1}^{K} \frac{u_k}{\sum_{m=1}^{M_c} \log_2(M_{k,m}) + w_k} \tag{20}$$

$$\text{subject to (C1) } \sum_{m=1}^{M_c} p_{k,m} \le P, \ \forall k \in \{1, 2, \cdots, K\}$$

$$\text{(C2) } \text{SER}_{k,m} \le \text{SER}_{\text{target}}, \ p_{k,m} \ge 0, \ M_{k,m} \in \mathcal{M}_A.$$

$$\forall k \in \{1, 2, \cdots, K\}, \ \forall m \in \{1, 2, \cdots, M_c\}$$

where (C1) is the total power constraint for each D2D transmitter, and (C2) is the SER constraint for each subcarrier of each D2D pair that is required for video delivery with no retransmission. We omit $\{v_k\}$ in (20), since $\{v_k\}$ are constant terms in the objective function.

### B. Proposed Resource Allocation Algorithm

Since constraint (C2) in (20) is not a convex set and thereby the optimization problem in (20) is NP-hard, we propose an iterative algorithm as a heuristic solution, which updates both the subcarrier assignment and the power allocation based on the CSI and the RD function.

Our proposed algorithm is initialized by multi-user diversity (MUD), where each subcarrier is assigned to the D2D pair with the best channel gain. Next, inspired by the equal slope condition for video multiplexing [32], we consider the D2D pair which has the steepest slope on the RD curve, and attempt to assign an additional subcarrier to this chosen D2D pair. The next step is to iterate over all subcarriers and iterate over all supported alphabet sizes for the chosen D2D pair. In the iteration, the minimal transmission power of the chosen D2D pair is calculated for each supported alphabet size on the current subcarrier via a bisection search, using either the proposed SER expression (18) or the SER obtained by the GA (9). For other D2D pairs on the current subcarrier, we also run an exhaustive search based on (18) or (9) for the largest alphabet sizes that satisfy the SER target under the interference from the chosen D2D pair. Afterwards, if the total MSE decreases, and the total transmission power of the chosen D2D pair does not exceed the power constraint, we update the transmission power, alphabet sizes and subcarrier assignment. This procedure is repeated iteratively until the total MSE of the video will not decrease by assigning one additional subcarrier to any D2D pair. The details of the proposed algorithm are summarized in Algorithm 1, while the MUD-based algorithm is given in Algorithm 2 as a baseline.

As a summary, to compare the proposed SER expression (18) and the SER obtained by the GA (9) for resource allocation, the majority of the Algorithm 1 is kept the same. The steps to use each of the SER evaluation methods are the bisection search for the minimal transmission power and the exhaustive search for the largest alphabet size in Algorithm 1.

---

**Algorithm 1** Proposed subcarrier and power allocation
---
Initialize $\{\rho_m\}$ and $\{M_{k,m}\}$ by MUD from Algorithm 2.
Bisection search for the minimal power $\{p_{k,m}\}$ for $\{M_{k,m}\}$.
Set the potential set $\Omega \leftarrow \{1, 2, \cdots, K\}$.
Calculate the current total video MSE $\{D_{\text{total}}^{(\text{current})}\}$ using (5).
**repeat**
    Calculate the slopes of the RD curves $\{S_k\}$ using (6).
    Choose the D2D pair $k^* \leftarrow \arg\min_{k \in \Omega}\{S_k\}$.
    **for** $m = 1$ to $M_c$ **do**
        **for** $n = 1$ to $N_A$ **do**
            Bisection search for the minimal power $\hat{p}_{k^*,m}[n]$
            of alphabet size $\mathcal{M}_n$ for D2D pair $k^*$.
            Exhaustive search for the largest alphabet size
            for each D2D pair in set $\rho_m$.
            Calculate the corresponding total video MSE
            $\{D_{\text{total}}[n]\}$ using (5).
        **end for**
        Set $n^* \leftarrow \arg\min_{n=\{1,2,\cdots,N_A\}}\{D_{\text{total}}[n]\}$
        **if** $D_{\text{total}}[n^*] < D_{\text{total}}^{(\text{current})}$, $\hat{p}_{k^*,m}[n^*] + \sum_{m'=1}^{M_c} p_{k^*,m'} \le P$ **then**
            Update $p_{k^*,m} \leftarrow \hat{p}_{k^*,m}[n^*]$ and $\rho_m \leftarrow \rho_m \cup k^*$.
            Update the alphabet sizes for D2D pairs in $\rho_m$.
            Exit the loop for $m$.
        **else if** $m = M_c$ **then**
            Set $\Omega \leftarrow \Omega \backslash k^*$.
        **end if**
    **end for**
**until** $\Omega$ is empty
---

**Algorithm 2** MUD-based subcarrier and power allocation
---
**for** $m = 1$ to $M_c$ **do**
    Choose the set of D2D pairs allocated to subcarrier $m$
    as $\rho_m \leftarrow \{\arg\max_{k \in \{1,2,...,K\}}(|h_m^{k,k}|)\}$
**end for**
**for** $k = 1$ to $K$ **do**
    Find $\{M_{k,m}\}$ and $\{p_{k,m}\}$ by water-filling [21].
**end for**
---

## V. RESULTS AND DISCUSSION

### A. Numerical Results for the SER of a D2D Receiver

In this section, we investigate the SER of a D2D receiver in the CCI using the proposed SER expression. A raised-cosine pulse with roll-off factor 0.5 is used in numerical results.

First, the proposed SER expression is corroborated by simulation. Fig. 2 shows the SER versus SNR for the 4-QAM desired signal and a 16-QAM CCI signal at SIR= 10dB and SIR = 15dB. The solid lines stand for the SERs obtained using the proposed expression (18) with $L = 20$, and the crosses denote the SERs obtained by Monte Carlo simulation. In the simulation, each data point is generated by averaging over $10^9$ symbols. We observe that the analytical results are in excellent agreement with the simulation. Therefore, we only show the results obtained by the analytical expression with $L = 20$ in the remaining examples.
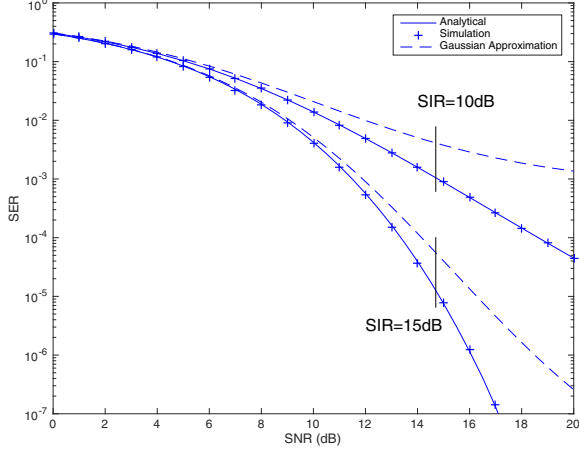
Fig. 2: SER versus SNR for the 4-QAM desired signal and one 16-QAM CCI signal at SIR= 10dB and 15dB.
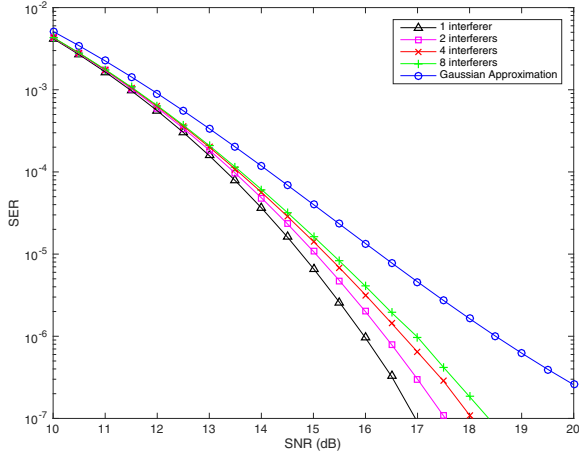


Fig. 3: SER versus SNR for one interferer and multiple interferers with equal received interference power at SIR = 15dB. The desired and the interference signals are modulated by 4-QAM and 16-QAM, respectively.

Next, we consider the SER under multiple interferers with equal received interference power. Fig. 3 presents that SER for a fixed received SIR when letting the interference power be equally distributed among all received interference signals. We observe from Fig. 3 that the SER increases as the number of CCI signals increases, and the gap between the analytical SER result and the SER obtained by the GA becomes smaller, which is an obvious consequence of the central limit theorem.

Finally, we assess the accuracy of the GA for the interference by comparing the resultant SER with the exact SER result. From Figures 2 and 3, it is observed that the GA overestimates the SER for QAM under the CCI. The gap between the GA and the exact SER is negligible at low SNR, but the gap is significant for high SNR. For example, when the SER target equals $10^{-3}$ and SIR=10dB, a SNR gap that is larger than 5dB is observed in Fig. 2 between the exact
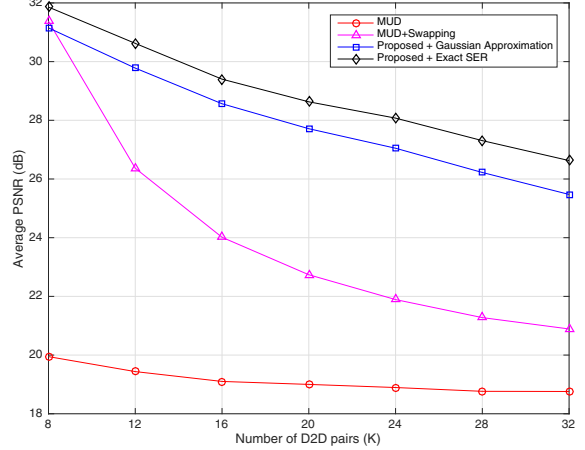


Fig. 4: Average video PSNR versus the number of D2D pairs for the proposed algorithms with the GA or the exact SER, compared with baseline algorithms.

SER expression and the GA. This behavior can be explained as follows: For given channel gains, the CCI at the output of the matched filter is bounded, if a raised cosine pulse with a non-zero roll-off factor is used. However, the GA generates an unbounded tail for the interference, which significantly overestimates the SER at high SNR.

B. Results of Resource Allocation for D2D Video Transmission

We simulate a D2D system with $M_c = 8$ subcarriers, each with bandwidth 15kHz. The roll-off factor for the RC pulse is $\beta = 0.5$, and the symbol rate is $1/T = 10$kHz. The channel response consists of path loss, shadowing and multi-path fading. The path loss is $46.8 + 18.7\log_{10}(d[m])$ and the shadowing follows a log-normal distribution with standard deviation of 3dB [33]. The subcarriers experience independent Rayleigh fading due to multipath, and the channel response is assumed to be flat within a subcarrier. The two-sided noise power spectral density is $-174$dBm/Hz. The maximal transmission power for each D2D pair is 100mW. The SER target is $10^{-3}$ in the simulation. The supported modulation formats are 4-QAM, 16-QAM and 64-QAM. We consider multiple D2D pairs uniformly distributed in a cell of a radius of 500 meters. The D2D distance is restricted between 10 and 50 meters. We generate $10^3$ realizations of geographical locations in the simulation, each with independent channels.

We use a video sequence with a resolution of $640 \times 480$, encoded using H.264/SVC reference software JSVM version 9.19.15. The total length of the video is 30 seconds at 30 frames per second, and the video is organized in GOPs of 15 frames (I-P-P-P). We create application layer diversity among D2D pairs and the same average complexity over time for different D2D pairs by assigning random starting points of the same cyclic video to different D2D pairs. The $4 \times 4$ DCT coefficients for the MGS layer [27] of each macroblock are split with MGS vector $[1, 1, 2, 2, 2, 8]$. The video contents are protected by a rate $2/3$ punctured turbo code. Each packet consists of 300 bytes of FEC plus data bits. The video quality

is evaluated by peak signal-to-noise ratio (PSNR), which is defined by $\text{PSNR} = 10\log_{10}\frac{255^2}{\mathbb{E}[\text{MSE}]}$.

The performance of the proposed cross-layer algorithm is simulated combined with either the exact SER expression or the GA. Two baseline algorithms are also used for comparison. The first one is Algorithm 2, which only uses MUD; the second baseline algorithm is the cross-layer orthogonal subcarrier assignment algorithm from [21], which is initialized by MUD and iteratively swaps the subcarrier assignment, namely "MUD+Swapping". The proposed resource allocation algorithm significantly outperforms the baseline algorithms by a 5dB PSNR gap for 20 to 32 D2D pairs. In Fig. 4, the PSNR gap between the proposed SER expression and the GA is approximately 1dB. When the proposed resource allocation algorithm with the GA admits 24 users with an average PSNR of approximately 27dB, the same algorithm with the proposed SER expression supports 30 users at the same average PSNR.

## VI. Conclusion

For a multicarrer D2D video transmission system, considerable improvement on user capacity and video quality by the proposed cross-layer resource allocation using the newly-derived, analytical and exact SER expression for D2D systems with bandlimited QAM signaling is demonstrated by the simulation, compared to the same resource allocation algorithm using conventional SER evaluation method by treating the interference as a Gaussian RV and other baseline algorithms.

## References

[1] K. Doppler, M. Rinne, C. Wijting, C. Ribeiro, and K. Hugl, "Device-to-device communication as an underlay to LTE-advanced networks," *IEEE Commun. Mag.*, vol. 47, no. 12, pp. 42–49, Dec. 2009.

[2] G. Wunder, P. Jung, M. Kasparick, T. Wild, F. Schaich, Y. Chen, S. Brink, I. Gaspar, N. Michailow, A. Festag *et al.*, "5GNOW: non-orthogonal, asynchronous waveforms for future mobile applications," *IEEE Commun. Mag.*, vol. 52, no. 2, pp. 97–105, Feb. 2014.

[3] J. van de Beek and F. Berggren, "Out-of-band power suppression in OFDM," *IEEE Commun. Lett.*, vol. 12, no. 9, pp. 609–611, Sep. 2008.

[4] G. Cherubini, E. Eleftheriou, and S. Ölçer, "Filtered multitone modulation for very high-speed digital subscriber lines," *IEEE J. Sel. Areas Commun.*, vol. 20, no. 5, pp. 1016–1028, Jun. 2002.

[5] R. Wang, J. Zhang, S. Song, and K. Letaief, "QoS-aware channel assignment for weighted sum-rate maximization in D2D communications," in *Proc. IEEE Global Communications Conf. (GLOBECOM)*, Dec. 2015, pp. 1–6.

[6] W. Zhao and S. Wang, "Resource sharing scheme for device-to-device communication underlaying cellular networks," *IEEE Trans. Commun.*, vol. 63, no. 12, pp. 4838–4848, Dec. 2015.

[7] C.-H. Yu, K. Doppler, C. B. Ribeiro, and O. Tirkkonen, "Resource sharing optimization for device-to-device communication underlaying cellular networks," *IEEE Trans. Wireless Commun.*, vol. 10, no. 8, pp. 2752–2763, 2011.

[8] G. Yu, L. Xu, D. Feng, R. Yin, G. Y. Li, and Y. Jiang, "Joint mode selection and resource allocation for device-to-device communications," *IEEE Trans. Commun.*, vol. 62, no. 11, pp. 3814–3824, Nov. 2014.

[9] L. Wei, R. Hu, Y. Qian, and G. Wu, "Enable device-to-device communications underlaying cellular networks: challenges and research aspects," *IEEE Commun. Mag.*, vol. 52, no. 6, pp. 90–96, Jun. 2014.

[10] *Digital Video Broadcasting (DVB); Frame structure channel coding and modulation for a second generation digital transmission system for cable systems (DVB-C2)*, ETSI Std. EN 302 769, Rev. 1.3.1, Oct. 2015.

[11] M. Celebiler and G. Coupe, "Effects of thermal noise, filtering and co-channel interference on the probability of error in binary coherent PSK systems," *IEEE Trans. Commun.*, vol. 26, no. 2, pp. 257–267, Feb. 1978.

[12] N. Beaulieu and J. Cheng, "Precise error-rate analysis of bandwidth-efficient BPSK in Nakagami fading and cochannel interference," *IEEE Trans. Commun.*, vol. 52, no. 1, pp. 149–158, Jan. 2004.

[13] N. Beaulieu and A. Abu-Dayya, "Bandwidth efficient QPSK in cochannel interference and fading," *IEEE Trans. Commun.*, vol. 43, no. 9, pp. 2464–2474, Sep. 1995.

[14] J. Cheng, N. Beaulieu, and X. Zhang, "Precise BER analysis of dual-channel reception of QPSK in Nakagami fading and cochannel interference," *IEEE Commun. Lett.*, vol. 9, no. 4, pp. 316–318, Apr. 2005.

[15] C. Rivera and J. Ritcey, "Error probabilities for QAM systems on partially coherent channels with intersymbol interference and crosstalk," *IEEE Trans. Commun.*, vol. 46, no. 6, pp. 775–783, Jun. 1998.

[16] X. Liu and L. Hanzo, "Exact BER of rectangular-constellation quadrature amplitude modulation subjected to asynchronous co-channel interference and Nakagami-m fading," in *Wireless Communications and Networking Conference (WCNC), IEEE*, 2007, pp. 2216–2220.

[17] W. Yu and R. Lui, "Dual methods for nonconvex spectrum optimization of multicarrier systems," *IEEE Trans. Commun.*, vol. 54, no. 7, pp. 1310–1322, Jul. 2006.

[18] Z.-Q. Luo and S. Zhang, "Dynamic spectrum management: Complexity and duality," *IEEE J. Sel. Topics Signal Process.*, vol. 2, no. 1, pp. 57–73, Feb. 2008.

[19] T. Schierl, T. Stockhammer, and T. Wiegand, "Mobile video transmission using scalable video coding," *IEEE Trans. Circuits Syst. Video Technol.*, vol. 17, no. 9, pp. 1204–1217, Sep. 2007.

[20] M. van der Schaar, S. Krishnamachari, S. Choi, and X. Xu, "Adaptive cross-layer protection strategies for robust scalable video transmission over 802.11 WLANs," *IEEE J. Sel. Areas Commun.*, vol. 21, no. 10, pp. 1752–1763, Dec. 2003.

[21] D. Wang, L. Toni, P. Cosman, and L. Milstein, "Uplink resource management for multiuser OFDM video transmission systems: Analysis and algorithm design," *IEEE Trans. Commun.*, vol. 61, no. 5, pp. 2060–2073, May 2013.

[22] D. Wu, J. Wang, R. Hu, Y. Cai, and L. Zhou, "Energy-efficient resource sharing for mobile device-to-device multimedia communications," *IEEE Trans. Veh. Technol.*, vol. 63, no. 5, pp. 2093–2103, Jun. 2014.

[23] Q. Wang, W. Wang, S. Jin, H. Zhu, and N. T. Zhang, "Quality-optimized joint source selection and power control for wireless multimedia D2D communication using Stackelberg game," *IEEE Trans. Veh. Technol.*, vol. 64, no. 8, pp. 3755–3769, Aug. 2015.

[24] G. Fodor, E. Dahlman, G. Mildh, S. Parkvall, N. Reider, G. Miklós, and Z. Turányi, "Design aspects of network assisted device-to-device communications," *IEEE Commun. Mag.*, vol. 50, no. 3, pp. 170–177, Mar. 2012.

[25] N. Michailow, M. Matthé, I. S. Gaspar, A. N. Caldevilla, L. L. Mendes, A. Festag, and G. Fettweis, "Generalized frequency division multiplexing for 5th generation cellular networks," *IEEE Trans. Commun.*, vol. 62, no. 9, pp. 3045–3061, Sept. 2014.

[26] J. G. Proakis and M. Salehi, *Digital communications*, 5th ed. McGraw-Hill, New York, 2007.

[27] H. Schwarz, D. Marpe, and T. Wiegand, "Overview of the scalable video coding extension of the H.264/AVC standard," *IEEE Trans. Circuits Syst. Video Technol.*, vol. 17, no. 9, pp. 1103–1120, Sep. 2007.

[28] K. Stuhlmüller, N. Färber, M. Link, and B. Girod, "Analysis of video transmission over lossy channels," *IEEE J. Sel. Areas Commun.*, vol. 18, no. 6, pp. 1012–1032, Jun. 2000.

[29] N. Beaulieu, "A useful integral for wireless communication theory and its application to rectangular signaling constellation error rates," *IEEE Trans. Commun.*, vol. 54, no. 5, pp. 802–805, May 2006.

[30] P. Wu, P. C. Cosman, and L. B. Milstein, "Resource allocation for multicarrier device-to-device video transmission: Symbol error rate analysis and algorithm design," *submitted to IEEE Trans. Commun.*

[31] I. Gradshteyn and I. Ryzhik, *Table of integrals, series, and products*. Academic Press, 2007.

[32] A. Ortega, K. Ramchandran, and M. Vetterli, "Optimal trellis-based buffered compression and fast approximation," *IEEE Trans. Image Process.*, vol. 3, pp. 26–40, Jan. 1994.

[33] C. Xu, L. Song, and Z. Han, *Resource management for device-to-device underlay communication*. Springer, 2014.